Disorder-induced melting of the charge of the charge order in thin films of Pr0.5Ca0.5MnO3

Yang, Z.-Q.; Hendrikx, R.W.A.; Bentum, P.J.M. van; Aarts, J.

Disorder-induced melting of the charge order in thin films of $Pr_{0.5}Ca_{0.5}MnO_3$

2002 Europhys. Lett. 58 864

(http://iopscience.iop.org/0295-5075/58/6/864)

EUROPHYSICS LETTERS 15 June 2002

Europhys. Lett., **58** (6), pp. 864–870 (2002)

Disorder-induced melting of the charge order in thin films of $Pr_{0.5}Ca_{0.5}MnO_3$

Z. Q. Yang[1], R. W. A. Hendrikx[1], P. J. M. v. Bentum[2] and J. Aarts[1]

[1] *Kamerlingh Onnes Laboratory, Leiden University*
P.O. Box 9504, Leiden, the Netherlands
[2] *Nijmegen High Field Magnet Laboratory*
Toernooiveld 1, 6525 ED Nijmegen, the Netherlands

(received 20 December 2001; accepted in final form 29 March 2002)

PACS. 73.50.Fq – High-field and nonlinear effects.
PACS. 75.30.Vn – Colossal magnetoresistance.

Abstract. – We have studied the magnetic-field–induced melting of the charge order in thin films of $Pr_{0.5}Ca_{0.5}MnO_3$ (PCMO) films on $SrTiO_3$ (STO) by X-ray diffraction, magnetization and transport measurement. At small thickness (25 nm) the films are under tensile strain and the low-temperature melting fields are of the order of 20 T or more, comparable to the bulk value. With increasing film thickness the strain relaxes, which leads to a strong decrease of the melting fields. For a film of 150 nm, with in-plane and out-of-plane lattice parameters closer to the bulk value, the melting field has reduced to 4 T at 50 K, with a strong increase in the hysteretic behavior and also an increasing fraction of ferromagnetic material. Strain relaxation by growth on $YBa_2Cu_3O_{7-\delta}$ or by post-annealing yields even stronger reduction of the melting field. Apparently, strained films behave bulk-like. Relaxation leads to an increasing suppression of the CO state, presumably due to an atomic-scale disorder produced by the relaxation process.

Introduction. – The occurrence of charge order (CO) in doped perovskite manganites of type $RE_{1-x}A_xMnO_3$ (RE = trivalent rare earth, A = divalent alkaline earth) is currently a much studied phenomenon. The CO state, a long-range ordering of the Mn^{3+} and Mn^{4+} ions, is the result of a complicated competition between Coulomb interactions (between the charges), exchange interactions (between the Mn moments), and the electron-lattice coupling through Jahn-Teller distortions of the oxygen octhahedron surrounding the Mn^{3+}-ion. A favourable situation for CO is at $x = 0.5$, with equal amounts of Mn^{3+} and Mn^{4+} ions. The ordering is the CE-type checkerboard pattern, accompanied by orbital ordering of the e_g orbitals on the Mn^{3+} sites in a zigzag arrangement and, at lower temperatures, by antiferromagnetic ordering of the Mn moments [1–3]. The CO state has to compete with the charge-disordered ferromagnetic metallic (FM) state. For small deviations of the Mn-O-Mn bond angle from 180°, the band width W of the e_g electrons can be large, at least when the Mn core spins are aligned. The bond angles depend on the average radius of the RE and A ions, which means that a "large-W" system such as $Pr_{0.5}Sr_{0.5}MnO_3$ with decreasing temperature first goes into the FM state before the transition to the CO and antiferromagnetic (AFM) state takes place. For, *e.g.*, $Pr_{0.5}Ca_{0.5}MnO_3$, W is lower and CO occurs without

intervening FM state [4]. Even then, the AFM state at lower temperatures consists of FM zigzag chains, coupled in AFM fashion. The competition with the FM state also means that the CO state is sensitive to magnetic fields: it can "melt" into the metallic state by polarizing the Mn moments so that the band is formed. This magnetic-field–driven insulator-metal transition leads to a huge resistance decrease, which is one of the different types of "Colossal" magnetoresistance effects [5]. The field needed for the melting (at low temperatures) is again controlled by W, about 5 T for the (Pr,Sr) system, around 25 T for the (Pr,Ca) system, and even 60 T for $Sm_{0.5}Ca_{0.5}MnO_3$ [4]. Away from commensurate doping, the CE-type order is still the basic structure, but the CO state is less stable (lower melting fields) with tendencies to charge separation [6].

In thin-film form, the development and stability of the CO state has been much less studied, although, focusing on the $x = 0.5$ case, studies on different systems report an FM rather than a CO ground state [7, 8]. A special issue concerns the effects of strain. Given the strong electron-lattice coupling, it can be expected that strained films show properties different from the bulk materials. Strain should specifically be present in $Pr_{0.5}Ca_{0.5}MnO_3$ (pseudocubic lattice parameter $a = 0.381$ nm) grown on $SrTiO_3$ ($a = 0.391$ nm). Recently reported results on this combination demonstrated strongly reduced melting fields [9,10] for films in a thickness range of 75 nm–100 nm, which was ascribed to the fact that the distortions normally induced by the CO state cannot fully develop due to the strain imposed by the substrate.

In the present work, we report on a similar study on $Pr_{0.5}Ca_{0.5}MnO_3$ (PCMO) thin films of varying thickness, deposited on STO-[100] by dc magnetron sputtering, but we come to a different conclusion. At small thickness (25 nm) the strained films still require high CO melting fields H_m of the order of 20 T, quite close to the value of bulk single crystals [11]. With increasing film thickness, the strain relaxes but the bulk-like behavior is increasingly lost; still, in the thickness range around 80 nm, H_m is significantly higher than found in refs. [9,10]. At thicknesses around 150 nm the films are almost free of strain and H_m at 50 K has reduced to 4 T, with a strong increase in the hysteretic behavior and the appearance of a ferromagnetic signal. The data suggest that the strain itself does not impede formation of the CO state, but that the relaxation leads to the observed reduction of H_m, presumably due to the generation of lattice defects.

Experimental. – All films studied were sputter deposited from ceramic targets of nominally $Pr_{0.5}Ca_{0.5}MnO_3$ and $YBa_2Cu_3O_7$ on STO substrates, in a pure-oxygen atmosphere of 300 Pa with a substrate-source on-axis geometry and growth rates of 0.4 nm/min and 2.5 nm/min for PCMO and YBCO, respectively. We will denote samples by their thickness, P80 meaning a PCMO film of 80 nm. Bilayers were grown by rotating the sample from one target position to the other. The growth temperature was chosen at 840°C. The samples were cooled to room temperature after deposition without post-annealing, which leads to non-superconducting $YBCO_{7-\delta}$ with $\delta = 0.53$ (as determined from the lattice parameter). Magnetotransport up to 9 T and magnetization up to 5 T were measured with an automated measurement platform and a SQUID-based magnetometer. Measurements in fields above 9 T were performed in a Bitter magnet at the High Field Magnet Laboratory (Nijmegen). Lattice parameters were determined by X-ray diffraction, for out-of-plane from the $(010)_c$, $(020)_c$ and $(030)_c$ reflections (c refers to the pseudocubic cell, with the b-axis taken perpendicular to the substrate), for in-plane from the $(013)_c$ and $(023)_c$ reflections.

Results and discussion. – The structure of bulk PCMO is orthorhombic (*Pnma*) with $a = 0.5395$ nm, $b = 0.7612$ nm and $c = 0.5403$ nm [12]. In terms of a pseudocubic lattice parameter a_c, this means a slight difference between the (a, c)-plane ($a_c = 0.3818$ nm) and the b-axis ($a_c = 0.3806$ nm). Electron diffraction showed that for thin films (below roughly 80 nm)

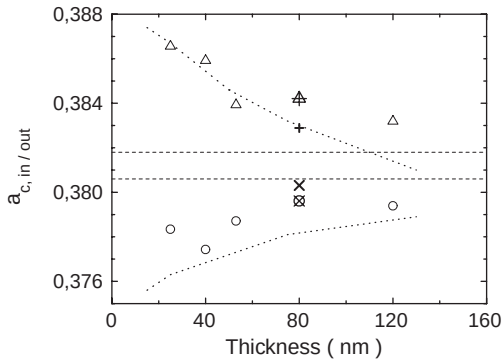

Fig. 1 – Lattice parameters (○ out-of-plane $a_{\mathrm{c,out}}$; △ in-plane $a_{\mathrm{c,in}}$) for films of $Pr_{0.5}Ca_{0.5}MnO_3$ with different thickness. The dotted lines show the behavior for $a_{\mathrm{c,in,out}}$ as found in ref. [9]. The horizontal dashed lines indicate the bulk values. The symbols circle/cross and triangle/plus denote a 1 hour post-annealed film of 80 nm; $(+, \times)$ denote the same film after a 5 h post-anneal.

the [010]-axis of the film is perpendicular to the substrate, in accordance with the findings of ref. [9]. For thick films (≈ 150 nm) the preferential orientation is the same, but domains with the [010]-axis in the substrate plane are also found. The thickness dependence of in-plane and out-of-plane lattice parameters $a_{\mathrm{c,in,out}}$ is plotted in fig. 1. At low thickness $a_{\mathrm{c,in}}$ is closer to the (larger) substrate value than to the bulk value, while $a_{\mathrm{c,out}}$ is smaller than the bulk value, indicating that the films grow epitaxially and strained. With increasing thickness both lattice parameters tend towards the bulk values. The behavior is quite similar to that reported in ref. [9] as indicated in fig. 1. The full width at half-maximum of the rocking curve of the (020) peak for all films is smaller than 0.5°, indicating good crystallinity.

All films showed semiconductor-like insulating behavior in zero applied magnetic field, as illustrated in fig. 2a, b for P80 and P150. An anomaly is present in the logarithmic derivative $\mathrm{d}R/\mathrm{d}(1/T)$ around a value expected for the CO transition temperature T_{CO}, but without the jump which is prominently observed in bulk material at 240 K. This absence is probably due to the fact that the increase of the in-plane lattice parameter which accompanies the charge ordering is already accommodated by the substrate strain [13]. The CO transition is visible in the magnetization M, especially for the thicker films. As shown in the inset of fig. 2b, $M(T)$ for P150 in a field of 1 T shows a clear shoulder around 240 K, reminiscent of the peak in the susceptibility found in the bulk material at T_{CO} (and above the magnetic transition) [14]. For films of 25 nm, the resistance drop in a magnetic field, which signifies the CO melting, was found at temperatures below 100 K near the maximum available field of 20 T for one sample, while a second one did not show a change in R up to 20 T. Also, $R(H)$ is hysteretic: upon decreasing the field the resistance jumps back up at a lower field, since the melting transition is first order. We denote the upper and lower melting fields as H_{m}^{+} and H_{m}^{-}, respectively. With increasing thickness, both branches shift to lower fields. Examples of $R(H)$ for P80 and P150 are given in fig. 2c, d. For P150, H_{m}^{+} has dropped to only 5 T around 50 K. The resistance changes are sharp, making H_{m} well defined, and the curves can be used to construct the temperature field phase diagrams [15] shown in fig. 3, where at zero field the value of the bulk is used. The shape of the phase diagrams changes significantly with increasing thickness. For P25, hysteresis is only present below 70 K in the field region 16 T–20 T. These large values resemble the numbers found for bulk single crystals. For P80, hysteresis starts below 130 K and the difference between the $(+, -)$ branches increase considerably, especially at low temperatures; the H_{m}^{+} branch is still above 12 T at all temperatures, which explains the

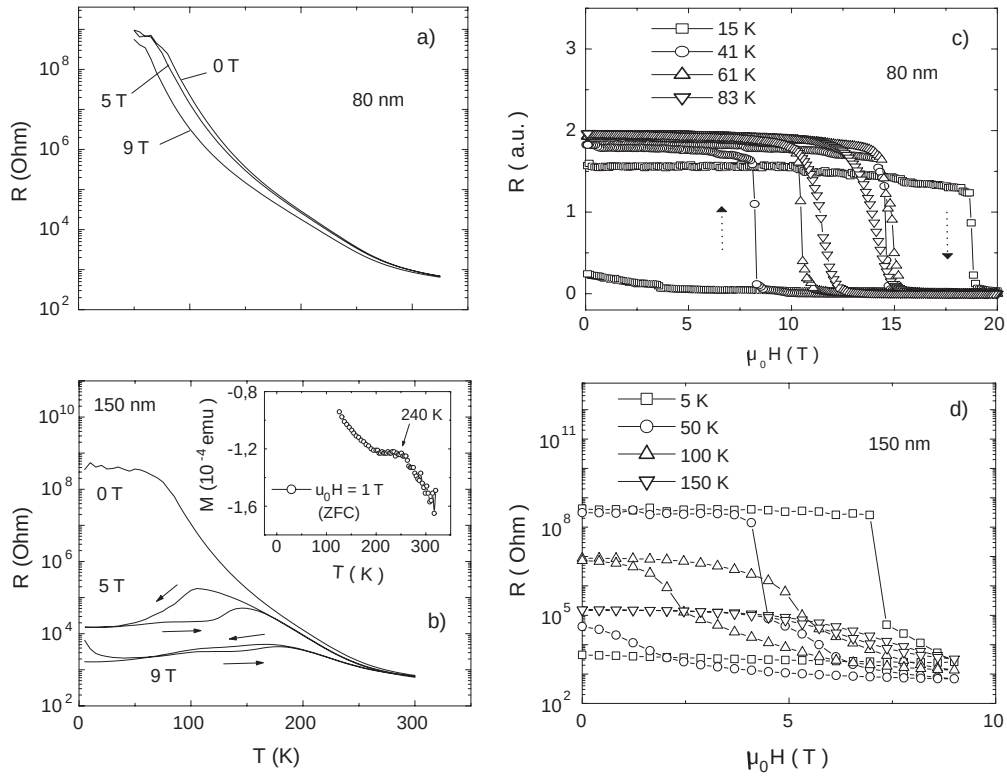

Fig. 2 – Resistance R *vs.* temperature T at magnetic fields $\mu_0 H = 0, 5, 9$ T for films of $Pr_{0.5}Ca_{0.5}MnO_3$ with thickness (a) 80 nm, (b) 150 nm; for the same films R *vs.* $\mu_0 H$ at different T as indicated, (c) 80 nm, (d) 150 nm. The insert in (b) shows the temperature-dependent magnetization, zero-field-cooled followed by warming in 1 T.

small MR effects seen in fig. 2a. Both $H_{\rm m}^{+}$ and $H_{\rm m}^{-}$ are considerably larger than reported in ref. [10]. In P150 hysteresis is found below 175 K. Both branches have shifted to lower fields: $H_{\rm m}^{+}$ is curved with a minimum value of 4 T around 50 K, while $H_{\rm m}^{-}$ now lies at zero field for temperatures below 80 K.

The melting transition is insulator-metal, but also antiferromagnetic-ferromagnetic, and can therefore be seen in the magnetization. Figure 4a shows $M(H)$ of P150 at 100 K, for the field sequence $0\,\mathrm{T} \rightarrow +5\,\mathrm{T} \rightarrow -5\,\mathrm{T} \rightarrow +5\,\mathrm{T}$, with the diamagnetic substrate signal subtracted. The sample was cooled down in zero field. A small ferromagnetic component is already present in this virgin state (indicated by $M_{\rm ZFC}$ in fig. 4); with increasing field, $M(H)$ is constant until 1.8 T, then rises significantly when the field is increased to 5 T. Upon decreasing the field, M now remains constant because the sample is in the FM state, but starts to drop around 3 T when $H_{\rm m}^{-}$ is crossed as can be seen in fig. 3c (dotted line). At zero field, the ferromagnetic component has grown by more than a factor 2. The same behavior is found when continuing the loop to -5 T; when going back up to $+5$ T, M merges with the virgin curve above 4 T.

The first conclusion we draw is that the CO state in the strained material is hardly less stable (if at all) than in the bulk. This is different from the one reached in refs. [9, 10], but it is in good agreement with the data reported on Cr-doped films [13]: in that case it was found that strain-free films very quickly developed ferromagnetism upon Cr doping, but that Cr-doped films under tensile strain were still insulating, suggesting that the strain counteracts

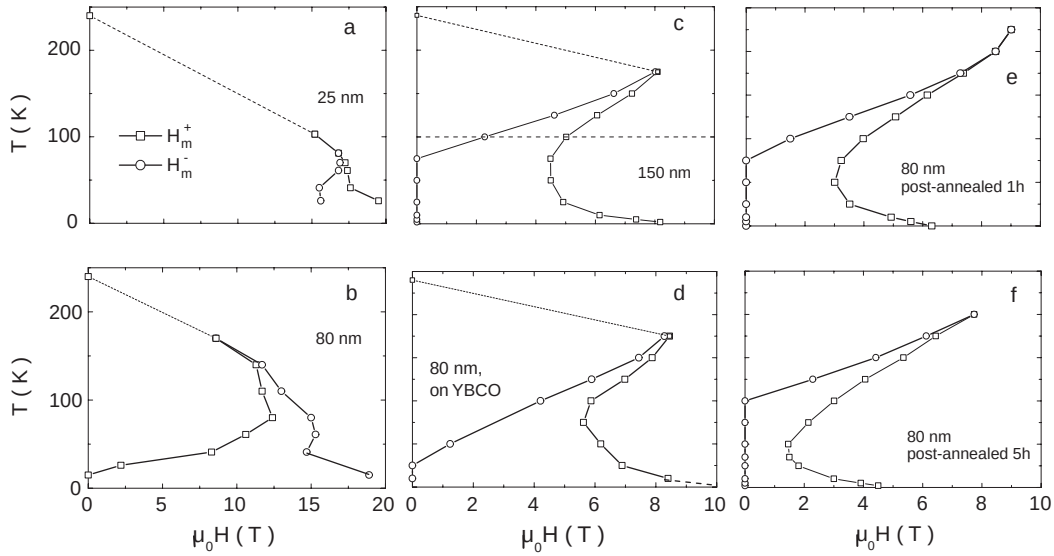

Fig. 3 – Charge order melting-field phase diagrams as determined from the magnetoresistance for films of different thickness. The point at zero field is the bulk value for T_{CO}. (a) 25 nm; (b) 80 nm; (c) 150 nm; (d) 80 nm, grown on YBCO template; (e) 80 nm post-annealed 1 h; (f) 80 nm post-annealed 5 h. The dashed line in (c) denotes the temperature of the magnetization measurements given in fig. 4.

the effects of the Cr doping and stabilizes the CO state. The decreasing stability of the CO state with increasing film thickness appears due to the strain relaxation rather than the strain itself. The picture arising then is that defects (disorder) induced by the growth and the relaxation destabilize CO, but that the strain itself has no destabilizing effect or even the opposite, which is quite reasonable in view of the fact that the necessary lattice distortion is already accommodated (also suggested in ref. [13]).

In order to highlight the effects of strain relaxation we performed two more experiments. One 80 nm film was annealed in the growth chamber for one hour at 950 °C in 1 mbar O_2 (the sputtering pressure) and slowly cooled; after measuring it was annealed for an additional

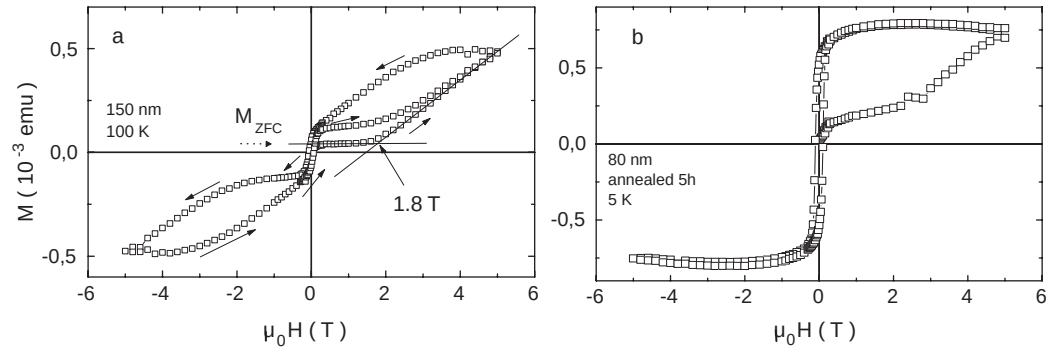

Fig. 4 – Magnetization M *vs.* magnetic field $\mu_0 H$ for films of $Pr_{0.5}Ca_{0.5}MnO_3$. In both cases, the magnetization of the substrate has been subtracted. (a) Film of 80 nm at 100 K. The magnetization found in low field after zero-field-cooling is denoted M_{ZFC}; (b) film of 80 nm, post-annealed for 5 h, at 5 K.

5 hours in flowing oxygen at 900 °C. Another 80 nm film was grown on a 10 nm YBCO template layer (called PY). Both methods effectively relax the strain in PCMO. Lattice parameter values ($a_{\mathrm{c,out}}$, $a_{\mathrm{c,in}}$) are (0.384 nm, 0.380 nm) for the 1 hour post-annealed sample, (0.383 nm, 0.380 nm) for the 5 hour post-annealed sample, and (0.385 nm, 0.380 nm) for PY, showing that all have undergone relaxation, especially in the out-of-plane axis. The CO-melting phase diagrams for these samples again show a strong decrease of the melting fields (see fig. 3d, f), with the 5 hour post-annealed sample reaching the lowest value yet observed in this system (1.5 T at about 50 K). The field dependence of the magnetization, *e.g.*, at 5 K (fig. 4b) accordingly shows an increase of M around 3 T (due to the bending back of the H_{m}^{+} branch), but no decrease of M from 5 T downward until the ferromagnetic hysteresis regime is entered, since H_{m}^{-} now lies at 0 T.

Together, the observations lead to the following picture. At small thickness the pseudomorphic epitaxial growth leads to a strained film without any apparent crystallographic disorder. The film (a, c)-plane coincides with the substrate plane which favours the formation of a CE-type CO state for two reasons: the necessary Jahn-Teller distortions of the oxygen squares are facilitated by the larger a- and c-axis; and the zigzag nature of the orbital order inhibits the build-up of in-plane strain along one of the axes. In contrast, in $La_{0.7}Ca_{0.3}MnO_3$ the absence of such intrinsic strain relief was found to lead to the formation of antiphase boundaries in very thin films [16]. It may even be surmised that the strain has a stabilizing effect on the CO state which offsets the unavoidable point disorder, leading to melting fields close to those of the bulk. Relaxation induces defects, which could be responsible for the change in melting behavior. Here it is important to note that the development of the phase diagrams with increasing relaxation closely resembles the changes found in the bulk when going from $x = 0.5$ (small hysteretic regime at a large field) to $x = 0.3$ (curved upper branch at low fields and lower branch going to zero) [5]; especially the similarity between the behavior of the 5 h post-annealed film and the $x = 0.3$ bulk material is striking, with both showing a minimum H_{m}^{+} field of about 2 T around 30-40 K, and the H_{m}^{-} branch at zero field. The re-entrant character of the CO state in the (T, H) phase diagram is due to the fact that the CO state has a larger entropy than the FM state [17]. In the bulk case for $0.3 < x < 0.5$, the deviation from commensurate doping leads to extra Mn^{3+} ions, which are apparently distributed in a random way in the commensurate CO matrix. In our films the amount of carriers is not changed but random structural disorder will have the same effect, reduced stability of the zigzag chains and less-than-full ordering, which yields extra entropy to the CO state. The nature of this partially ordered state might well be phase-separated, given the ferromagnetic tendencies of the system. We observe that the structure relaxation is accompanied by an increasing amount of ferromagnetic component in the magnetization, which could be either due to canting of the antiferromagnetically aligned moments or to ferromagnetic clusters. Finally, we note that disorder as a major source for reduced melting fields can explain the difference between our results and those of refs. [9,10] as caused by the different morphology of the sputtered *vs.* the laser-ablated films; and also the general difficulty in obtaining CO ground states in thin films: if CO films are to be grown, avoiding disorder is the major source of concern.

In summary, we have shown that the melting fields H_{m} for the insulating CO state in $Pr_{0.5}Ca_{0.5}MnO_3$ films under tensile strain are around 20 T or even above at low temperatures, rather close to the values found for the bulk material. Strain relaxation strongly reduces H_{m}. With increasing film thickness, the lattice parameters of the film demonstrate relaxation, while H_{m} decreases down to 4 T at 50 K for a 150 nm film. Upon strain relaxation by post-annealing this value becomes even smaller. We suggest this is due to induced defects, which destabilize the CO antiferromagnetic state and possibly even promote the formation of ferromagnetic clusters.

* * *

This work is part of the research program of the "Stichting voor Fundamenteel Onderzoek der Materie (FOM)", which is financially supported by NWO. We would like to thank H. W. Zandbergen and M. Y. Wu for electron microscopy characterisation.

REFERENCES

[1] Wollan E. O. and Koehler W. C., *Phys. Rev.*, **100** (1955) 545.
[2] v.d. Brink J., Khaliullin G. and Khomskii D., *Phys. Rev. Lett.*, **83** (1999) 5118.
[3] v. Zimmermann M., Hill J. P. Gibbs Doon, Blume M., Casa D., Keimer B., Murakami Y., Tomioka Y. and Tokura Y., *Phys. Rev. Lett.*, **83** (1999) 4872.
[4] Tokura Y. and Tomioka Y., *J. Magn. & Magn. Mater.*, **200** (1999) 1.
[5] Tokura Y., Tomioka Y., Kuwahara H., Asamitsu A., Moritomo Y. and Kasai M., *Physica C*, **263** (1996) 544.
[6] Dagotto E., Hotta T. and Moreo A., *Phys. Rep.*, **344** (2001) 1.
[7] Wagner P., Gordon I., Vantomme A., Dierickx D., van Bael M. J., Moshchalkov V. V. and Bruynseraede Y., *Europhys. Lett.*, **41** (1998) 49.
[8] Nyeanchi E. B., Krylov I. P., Zhu X.-M. and Jacobs N., *Europhys. Lett.*, **48** (1999) 228.
[9] Prellier W., Haghiri-Gosnet A. M., Mercey B., Lecoeur Ph., Hervieu M., Simon Ch. and Raveau B., *Appl. Phys. Lett.*, **77** (2000) 1023.
[10] Prellier W., Simon Ch., Haghiri-Gosnet A. M., Mercey B. and Raveau B., *Phys. Rev. B*, **62** (2000) R16337.
[11] Tokunaga M., Miura N., Tomioka Y. and Tokura Y., *Phys. Rev. B*, **57** (1998) 5259.
[12] Jirák Z., Krupicka S., Simsa Z., Doulka M. and Vratislav S., *J. Magn. & Magn. Mater.*, **53** (1985) 153.
[13] Ogimoto Y., Izumi M., Manako T., Kimura T., Tomioka Y., Kawasaki M. and Tokura Y., *Appl. Phys. Lett.*, **78** (2001) 3505.
[14] Jirák Z., Damay F., Hervieu M., Martin, Raveau B., André G. and Bourée F., *Phys. Rev. B*, **61** (2000) 1181.
[15] Tomioka Y., Asamitsu A., Kuwahara H., Moritomo Y. and Tokura Y., *Phys. Rev. B*, **53** (1996) R1689.
[16] Zandbergen H. W. , Freisem S., Nojima T. and Aarts J., *Phys. Rev. B*, **60** (1999) 10259.
[17] Khomskii D., *Physica B*, **280** (2000) 325.